Resolving Arterial Contributions in Vessel Encoding Dynamic Angiography

M. A. Chappell[1,2], T. W. Okell[1], P. Jezzard[1], and M. W. Woolrich[1]
[1]FMRIB Centre, University of Oxford, Oxford, United Kingdom, [2]Institute for Biomedical Engineering, University of Oxford, Oxford, United Kingdom

Introduction: Non-invasive dynamic angiography can be performed using an Arterial Spin Labelling (ASL) contrast [1]. Application of a vessel encoding variation (VE-ASL) [2] provides a method for vessel selective dynamic angiography [3]. This provides an alternative to the highly invasive intra-arterial contrast injection x-ray angiography. VE-ASL involves the spatial modulation of the ASL label over a series of acquisitions so that blood water in each artery is uniquely encoded, the contribution of each artery being disambiguated at the analysis stage. VE-ASL preparations often rely on spatial modulation of the label in left-right (LR) and anterior-posterior (AP) directions. For labelling of the cerebral arteries, it is not generally possible to separate more than three arterial contributions (e.g. both carotid arteries plus a single combination of the vertebral arteries) using only LR and AP encodings with an encoding matrix based analysis. Previous attempts have had to incorporate extra information, such as the assumption that carotid and vertebral territories are separate [4]. An alternative would be to use clustering methods, as demonstrated in perfusion VE-ASL [5,6]. That analysis method can separate more arterial contributions, however it is unable to separately estimate contributions in areas of overlap, a common feature in 2D angiographic images. Recently a general framework for VE-ASL perfusion analysis [7] has been demonstrated that employs classification to overcome the limitations on the number of arteries that can be identified that is imposed by a conventional acquisition. Here we modify this analysis for application to VE-ASL dynamic angiography and demonstrate separation of contributions from all four carotid and vertebral arteries.

Methods: The general framework for VE-ASL analysis was employed [7] for data analysis: the encoding process was described by an encoding matrix [2], where the entries were populated based on the known geometry of the labelled vessels obtained from a 3D time-of-flight acquisition. To account for arteries not being located at the nodes of the modulation and thus not being perfectly labelled or controlled, the modulation function was simulated from the Bloch equations assuming a mean flow speed of 30 cm/s and a parabolic flow profile. The rank of the encoding matrix precluded direct inversion to estimate contributions from all four arteries. The approach of [7] overcomes this problem by constraining the solution via a probabilistic classification, where locations (voxels) are classified into groups indicating which subset (pairs) of arteries feed that voxel. Thus the analysis constrains the solution at the same time as still allowing for locations that are fed by multiple vessels. Indeed, the use of a probabilistic (rather than hard) classification meant that it was still possible to resolve locations that were being fed by three or more arteries (e.g. in locations that have overlapping arteries apparent in the projected 2D angiographic images). Crucially, the analysis was modified to operate on the complex valued phase and magnitude images, rather than purely magnitude information commonly considered in ASL imaging. This was necessary since the phase of the blood and static tissue signals can differ significantly where the blood is accelerating, and also depends on the TI delay following tag inversion.

The vessel selective angiography sequence consisted of a VEPCASL pulse train [2] of 1000 ms duration followed by a two-dimensional thick-slab flow-compensated Fast Low Angle Shot (FLASH) readout combined with a segmented Look-Locker sampling strategy (temporal resolution = 55 ms) [8]. Selective labelling was performed at the level of the neck in a six-cycle experiment: non-selective tag, non-selective control, two complementary left-right encodings (tag left arteries, control right and vice versa) and two complementary anterior-posterior encodings (tag anterior arteries, control posterior and vice versa). Transverse, Coronal and Saggital views were acquired, the sagittal view was rotated by 13.5° about the superior-inferior axis (i.e. from a standard sagittal view towards a coronal view) to reduce the amount of overlap of the vessels in the projected image. The six cycles comprised three pairs of images; each pair contained a common static tissue signal and orthogonal vessel encoded label signal. As a pre-processing the pairs of images were subtracted to remove the static signal and reduce any effects of scanner drift.

Results: Angiograms in transverse, coronal and sagittal (oblique) planes for one subject are shown in Figure 1, along with maximum intensity projections (MIPs) from the time-of-flight (TOF) data for comparison. In this subject there was little mixing of the blood from the two vertebral arteries when they fuse to form the basilar artery, despite the blood moving to the contralateral side (white arrows), and only moderate mixing downstream in the posterior cerebral arteries (yellow arrows). Some collateral flow from the right internal carotid to the right posterior cerebral artery was visible in the transverse view (purple arrows). In the coronal view the external carotid arteries were also visible. Figure 2 shows that it is possible for subject specific mixing of vertebral blood in the basilar artery to be resolved, since in this subject almost complete mixing occurs by the time the blood reaches the posterior cerebral arteries (yellow arrows).

Discussion: Using a classification-based analysis for VE dynamic angiography permits contributions from both carotids and vertebral to be resolved from data containing only LR and AP encoded cycles. Such analysis cannot be performed by the conventional inversion of the encoding matrix since there is insufficient unique information provided from the 6 cycles (technically the matrix is rank deficient). An alternative is to collect further cycles of encoded data, however, to obtain the extra unique information required, these must be oblique to the LR and AP directions (for common vessel geometries). Even if such data were available the classification analysis can achieve better noise suppression through considering sub-matrices of the full encoding matrix in turn [7]. The current implementation of the classification analysis requires fairly computational expensive calculations, a disadvantage compared to simple matrix inversion. However, further refinement of the technique should result in an algorithm appropriate for clinical application.

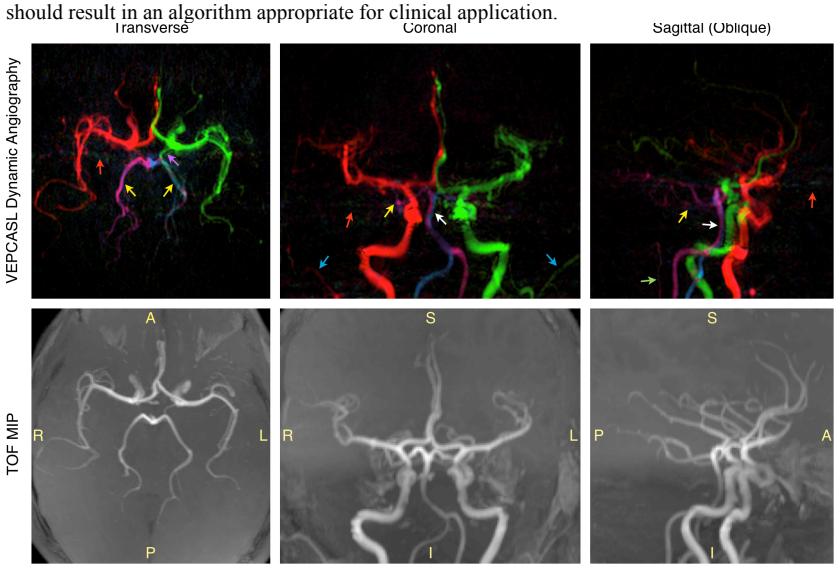

Figure 1: Vessel-selective dynamic angiography images (top row) in the same subject. Time-of-flight maximum intensity projections are also shown (bottom row). Features of interest include: little mixing of vertebral blood in the basilar artery despite the blood moving to the contralateral side (white arrows), even downstream in the posterior cerebral arteries (yellow arrows); collateral flow from the right internal carotid to the right posterior cerebral artery (purple arrow); external carotid arteries (blue arrows); the left posterior inferior cerebellar artery (green arrow); and a small amount of residual background signal in some areas (red arrows).

Figure 2: Vessel selective dynamic angiography data in a coronal view for a second subject. In this subject the blood from the two vertebral arteries is relatively mixed by the time it reaches the posterior cerebral arteries (yellow arrows).

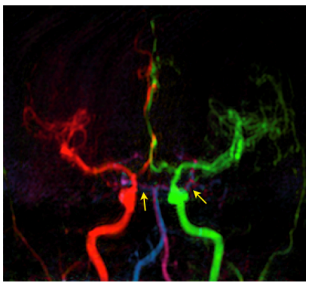

References:
1. Edelamn *et al.* Magn Reson Med 1994. 31:233-8.
2. Wong, E.C., Magn Reson Med, 2007. 58:1086-91.
3. Okell, T.W., *et al*, in Proc ISMRM Honolulu, 2009
4. Kansagra *et al*,. JMRI, 2008
5. Wong, E.C. *et al.*, in Proc. ISMRM Toronto, 2008
6. Kansagra *et al*., in Proc. ISMRM Hawaii, 2009.
7. Chappell *et al.*, this meeting,
8. Gunther, M., *et al.*, Magn Reson Med 2001. 46:974-984